On large N limit of symmetric traceless tensor models

Igor R. Klebanov[a,b] **and Grigory Tarnopolsky**[a]

[a]*Department of Physics, Princeton University,*
Princeton, NJ 08544, U.S.A.

[b]*Princeton Center for Theoretical Science, Princeton University,*
Princeton, NJ 08544, U.S.A.

E-mail: klebanov@Princeton.edu, grtarnop@gmail.com

ABSTRACT: For some theories where the degrees of freedom are tensors of rank 3 or higher, there exist solvable large N limits dominated by the melonic diagrams. Simple examples are provided by models containing one rank 3 tensor in the tri-fundamental representation of the $O(N)^3$ symmetry group. When the quartic interaction is assumed to have a special tetrahedral index structure, the coupling constant g must be scaled as $N^{-3/2}$ in the melonic large N limit. In this paper we consider the combinatorics of a large N theory of one fully symmetric and traceless rank-3 tensor with the tetrahedral quartic interaction; this model has a single $O(N)$ symmetry group. We explicitly calculate all the vacuum diagrams up to order g^8, as well as some diagrams of higher order, and find that in the large N limit where $g^2 N^3$ is held fixed only the melonic diagrams survive. While some non-melonic diagrams are enhanced in the $O(N)$ symmetric theory compared to the $O(N)^3$ one, we have not found any diagrams where this enhancement is strong enough to make them comparable with the melonic ones. Motivated by these results, we conjecture that the model of a real rank-3 symmetric traceless tensor possesses a smooth large N limit where $g^2 N^3$ is held fixed and all the contributing diagrams are melonic. A feature of the symmetric traceless tensor models is that some vacuum diagrams containing odd numbers of vertices are suppressed only by $N^{-1/2}$ relative to the melonic graphs.

KEYWORDS: 1/N Expansion, Conformal Field Theory, Nonperturbative Effects

ARXIV EPRINT: 1706.00839

Contents

1 Introduction and summary

Large N tensor models were introduced in the early 1990s [1–3] in an attempt to extend the correspondence of large N matrix models and two-dimensional quantum gravity to dimensions higher than two. These early papers contained many new insights, including the importance of the particular quartic interaction vertex for rank-3 tensors, where every pair of fields have only one index in common:

$$V_4 = \frac{3g}{2} \phi^{abc} \phi^{ade} \phi^{fbe} \phi^{fdc} \ . \tag{1.1}$$

Integral over the tensor with a quadratic term and this quartic interaction is not well-defined non-perturbatively because V_4 is not bounded from below. However, it may be formally expanded in powers of g; then it generates dynamical gluing of tetrahedra and was viewed as a step towards understanding 3-dimensional quantum gravity.

The models considered originally involved tensors with indices transforming under a single symmetry group, $\mathrm{SU}(N)$ or $O(N)$, but the large N limit appeared to be difficult to analyse in such models. Years later it was understood that, if the theory has multiple symmetry groups, and the 3-tensors are in tri-fundamental representations, then there is an exactly solvable large N limit where $g^2 N^3$ is held fixed [4–11]. Dominant in this limit are the so-called melonic Feynman diagrams (see figure 1), which are obtained by iterating the insertion of a two-loop sunset graph into each propagator (this class of diagrams was also studied in the early papers [12, 13]). The melonic diagrams constitute a small subset of the total number of diagrams (it is considerably smaller than the planar diagrams that dominate in the 't Hooft large N limit [14], which is used in the matrix models [15]), and this accounts for the exact solvability of the theories. Recently there has been a renewed interest in the theories with tensor degrees of freedom due to their connection [16, 17] with the SYK-like models of fermions with disordered couplings [18–25].
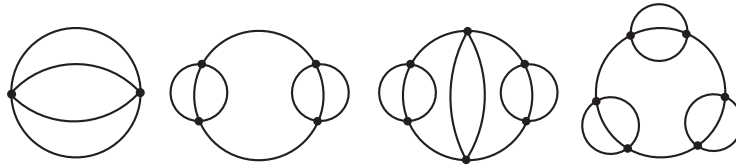
Figure 1. All the melonic vacuum diagrams up to order g^6.

A class of theories where such a melonic large N limit has been proven to exist have $O(N)^3$ symmetry with a real 3-tensor in the tri-fundamental representation [11, 17]. In other words, the 3 indices of a tensor are distinguishable, and each one is acted on by a different $O(N)$ group:

$$\varphi^{abc} \to M_1^{aa'} M_2^{bb'} M_3^{cc'} \varphi^{a'b'c'}, \tag{1.2}$$

$$M_1 \in O(N)_1, \quad M_2 \in O(N)_2, \quad M_3 \in O(N)_3. \tag{1.3}$$

For such theories one can draw the stranded graphs using the triple-line notation (we may draw each propagator as containing strands of three different colors), and it is possible to prove the melon dominance. In particular, all odd orders of perturbation theory are suppressed in the large N limit [11, 17]. A useful step in the proof is to imagine erasing all the loops of a given color, i.e. corresponding to one of the $O(N)$ groups, and then counting the remaining loops in the double-line graphs using their topology.

Such a method is not available, however, for a theory where there is only one $O(N)$ symmetry group, and the real tensor is in its 3-index irreducible representation (for example, the fully symmetric traceless one or the antisymmetric one).[1] In [17] we carried out some perturbative checks of the melonic large N limit in such tensor models with interaction (1.1).[2] In this paper we report on a complete study of the combinatorial factors of the vacuum diagrams in the theory of a real symmetric traceless tensor up to order g^8, as well as some partial results at higher orders. For generating and drawing all diagrams we used the Mathematica program developed in [28]. We compare with corresponding explicit results for the theory with $O(N)^3$ symmetry where the real tensor has distinguishable indices. We find that the melonic diagrams are dominant in both models. While individual non-melonic diagrams are sometimes enhanced in the $O(N)$ model compared to the $O(N)^3$ model, these enhancements fall short of making them comparable with the melonic diagrams.

For the vacuum diagrams with even numbers of vertices, the melonic diagrams scale as $g^{2n}N^{3n+3}$, and we have checked up to $n=4$ that all other diagrams are suppressed at least by a factor of $1/N$ (we have also checked that this holds for some selected diagrams of order higher than g^8). These corrections are present in both the $O(N)^3$ and $O(N)$ models, and there are more contributing diagrams in the latter case. The vacuum diagrams with odd numbers of vertices behave differently in the two models. The maximum scaling of a graph with $2n+1$ vertices in the $O(N)^3$ model is $g^{2n+1}N^{3n+3}$, which implies a suppression

---

[1]Another interesting model is that of D Hermitian matrices with $U(N) \times O(D)$ symmetry. Although the standard technique of erasing all the loops of a given color is not applicable to this model, it was argued to be dominated by the melonic diagrams in the limit where N and D become large [26].

[2]The counting of $O(N)$ singlet operators in free theories of this type was carried out in [27].

Figure 2. Leading melonic propagator corrections in the $O(N)^3$ and $O(N)$ theories.

by $N^{-3/2}$ compared to the melonic graphs. In the $O(N)$ model the maximum scaling is $g^{2n+1}N^{3n+4}$, which implies a suppression by only $N^{-1/2}$ compared to the melonic graphs. Thus, the effective coupling parameter in the $O(N)$ model is of order $N^{-1/2}$, while in the $O(N)^3$ model it is of order $1/N$. This should have interesting implications for the structure of the large N limit.

Based on our explicit calculations of combinatorial factors, we conjecture that the model of a 3-index symmetric traceless tensor possesses a smooth large N limit where g^2N^3 is held fixed and all the contributing diagrams are melonic. As discussed in section 5, this limit is closely related to the one in the $O(N)^3$ model.

2 Large N scaling in $O(N)$ and $O(N)^3$ tensor models

In this section we calculate some combinatorial factors for different diagrams in $O(N)^3$ and $O(N)$ symmetric theories. For the $O(N)^3$ theory we normalize the interaction vertex as

$$\frac{\tilde{g}}{4}\varphi^{a_1b_1c_1}\varphi^{a_1b_2c_2}\varphi^{a_2b_1c_2}\varphi^{a_2b_2c_1}\,, \tag{2.1}$$

and take the propagator as

$$\langle\varphi^{abc}\varphi^{a'b'c'}\rangle_0 = \delta^{aa'}\delta^{bb'}\delta^{cc'}\,. \tag{2.2}$$

The stranded graph for the leading two-loop correction to the propagator is shown in figure 2. Since there are three index loops (one of each color), this graph is of order $\tilde{g}^2N^3$, and this is the quantity that should be held fixed in the large N limit.[3] More precisely, the two-point function including this graph is

$$\langle\varphi^{abc}\varphi^{a'b'c'}\rangle = \delta^{aa'}\delta^{bb'}\delta^{cc'}(1 + \tilde{g}^2N^3 + \dots)\,. \tag{2.3}$$

In the $O(N)$ model, where the tensor is fully symmetric and traceless, the propagator is

$$\langle\phi^{abc}\phi^{a'b'c'}\rangle_0 = \frac{1}{6}\Big(\delta^{aa'}\delta^{bb'}\delta^{cc'} + \delta^{ab'}\delta^{bc'}\delta^{ca'} + \delta^{ac'}\delta^{ba'}\delta^{cb'} + \delta^{ab'}\delta^{ba'}\delta^{cc'} + \delta^{ac'}\delta^{bb'}\delta^{ca'}$$

$$+ \delta^{aa'}\delta^{bc'}\delta^{cb'} - \frac{2}{N+2}\big(\delta^{ab}\delta^{ca'}\delta^{b'c'} + \delta^{ab}\delta^{cb'}\delta^{a'c'} + \delta^{ab}\delta^{cc'}\delta^{a'b'} + \delta^{ac}\delta^{ba'}\delta^{b'c'}$$

$$+ \delta^{ac}\delta^{bb'}\delta^{a'c'} + \delta^{ac}\delta^{bc'}\delta^{a'b'} + \delta^{bc}\delta^{aa'}\delta^{b'c'} + \delta^{bc}\delta^{ab'}\delta^{a'c'} + \delta^{bc}\delta^{ac'}\delta^{a'b'}\big)\Big)\,. \tag{2.4}$$

---

[3]The correction to two-point function coming from contracting two fields from the same vertex, i.e. the snail diagram, is of order gN. Since this is suppressed in the large N limit where $g \sim N^{-3/2}$, we will ignore the snail diagrams throughout the paper. Had we not imposed the tracelessness condition on the tensor, there would be diagrams containing multiple snail insertions which would violate the melonic limit (we are grateful to F. Ferrari and R. Gurau for pointing this out).

The structure of the melonic two-loop propagator correction in the $O(N)$ model is similar to that in the $O(N)^3$ model (see the stranded diagrams in figure 2).[4] We again find three additional index loops which contribute the factor $\sim N^3$. Thus, for the $O(N)$ model a plausible large N limit is with $g^2 N^3$ held fixed. More precisely, we find that the leading melonic propagator correction in the $O(N)$ theory is

$$\langle \phi^{abc} \phi^{a'b'c'} \rangle = \langle \phi^{abc} \phi^{a'b'c'} \rangle_0 (1 + g^2 N^3 + \dots) . \tag{2.5}$$

Note that we have normalized the coupling constant in the $O(N)$ theory as in (1.1), which differs by a factor 6 from the normalization in the $O(N)^3$ theory. The advantage of this normalization is that the coefficient in (2.5) is the same as in (2.3).

To compute the combinatorial factor of each graph in the $O(N)^3$ theory we represent the tetrahedral vertex as

$$\varphi^{abc} \varphi^{ade} \varphi^{fbe} \varphi^{fdc} = \delta^{aa'} \delta^{bb'} \delta^{cc'} \delta^{dd'} \delta^{ff'} \delta^{ee'} \, \varphi^{abc} \varphi^{a'de} \varphi^{fb'e'} \varphi^{f'd'c'} . \tag{2.6}$$

Then for a given graph, contracting fields using the propagator (2.2) and the 4! symmetric configurations of the vertex (2.6) one obtains a sum of products of the Kronecker delta symbols. Contracting the delta symbols one finds a polynomial in N. For the $O(N)$ theory the procedure is similar. We may continue to use the vertex (2.6) because the $O(N)$ propagator (2.4) implements symmetrization of the tensor indices. For example, an explicit evaluation of the melonic vacuum diagram with 2 vertices gives

$$\frac{\tilde{g}^2}{8}(N^6 + 3N^4 + 2N^3) \tag{2.7}$$

in the $O(N)^3$ model and

$$\frac{1}{48} g^2 \frac{(N-2)(N-1)N(N+4)\left(N^5 + 17N^4 + 98N^3 + 112N^2 - 576N - 768\right)}{(N+2)^3} \tag{2.8}$$

in the $O(N)$ model.

The fact that each propagator in the $O(N)^3$ model is made of three strands of different colors make it obvious that two different strands of a propagator cannot belong to the same loop. In the $O(N)$ model two different strands of a propagator may not belong to the same loop due to the condition that the tensor is traceless. Cutting a propagator of a vacuum graph therefore decreases the number of index loops by 3 and gives a graph contributing to the two-point function. This shows that each graph contributing to the two-point functions scales as the corresponding vacuum graph times N^{-3}.

We would like to prove that the melonic graphs dominate in the large N limit of $O(N)$ theory where $g^2 N^3$ is held fixed. While we don't know how to do this in general, we have shown that this is the case for all the vacuum diagrams up to order g^8, and some selected graphs of higher orders. We exhibit their pictures and the leading scaling with N in the

---

[4]In figure 2 no two distinct index loops wrap the same cycle of the unstranded ϕ^4 diagram. This is a general property of the theory with the tetrahedron vertex (1.1).

figures.[5] For each diagram the upper integer, shown in black, gives the leading power of N we find in the $O(N)$ model; the lower integer, shown in blue, gives the leading power we find in the $O(N)^3$ model. If a label B appears below, this means that the diagram is bi-partite, i.e. it appears in the theory where there are two types of vertices, and each propagator connects different vertices.

In our list of vacuum diagrams we omit the so-called cut vertex diagrams, i.e. the ones that become disconnected if a vertex and the 4 propagators leading to it are erased. They may also be viewed as (dressed) snail diagrams, i.e. the ones coming from the "figure eight" graph with the bare propagators replaced by the fully dressed ones. All such diagrams may be constructed out of a pair of vacuum diagrams by cutting a propagator in each, and then gluing them together using the tetrahedron vertex. Let us show that this always produces a graph which is suppressed compared to the melonic ones. Suppose the two original graphs are of order $g^{m_1}N^{n_1}$ and $g^{m_2}N^{n_2}$, respectively. When we cut a propagator in each of the two graphs, we lose a total of 6 index loops (for the symmetric tensor this is true only if the tracelessness is imposed). After gluing the two cut graphs into one with the tetrahedron vertex we can recover 4 index loops, but not more. For example, in the $O(N)^3$ theory we can make two additional green loops, but only one red and one blue loop (or an analogous stranded graph with colors permuted). In the theory of a symmetric traceless tensor we can also recover at most 4 index loops. So, the highest possible scaling of the combined graph is $N^{n_1+n_2-2}g^{m_1+m_2+1}$. Even if the two original graphs are melonic, i.e. $n_i = 3 + 3m_i/2$, the combined cut vertex graph scales as $N^3(gN^{3/2})^{m_1+m_2}(gN)$. It is suppressed by $N^{-1/2}$ in the melonic limit.[6]

The first difference in large N scaling between the $O(N)$ and $O(N)^3$ models appears in the diagram of order g^3, whose stranded versions are exhibited in figure 3. The diagram in the $O(N)^3$ theory has 6 loops and scales as g^3N^6; in the melonic limit this is $\sim N^{-3/2}$. The diagram in the $O(N)$ theory has 7 loops and scales as g^3N^7; in the melonic limit this is $\sim N^{-1/2}$. These expectations are confirmed by the exact evaluation of the cubic diagram:

$$\frac{1}{2}\tilde{g}^3 \left(N^6 + 3N^5 + 3N^4 + 2N^3\right) \tag{2.9}$$

in the $O(N)^3$ model, and

$$\frac{1}{24}g^3\frac{(N-2)(N-1)N(N+4)}{(N+2)^5}\Big(N^8 + 29N^7 + 286N^6 + 796N^5 - 3120N^4$$
$$- 15232N^3 + 12640N^2 + 78208N + 58368\Big) \tag{2.10}$$

in the $O(N)$ model. Thus, even though this diagram is enhanced by N in the $O(N)$ theory, it is still suppressed in the melonic large N limit.

---

[5]For each diagram not containing snail insertions, the dominant term at large N is not affected by the 9 terms $\sim 1/(N+2)$ which make the propagator (2.4) traceless. Keeping only the six leading terms in the propagator makes the computer calculation much less time and memory intensive.

[6]If the two cut graphs are glued with the pillow vertex $g_p\varphi^{a_1b_1c_1}\varphi^{a_1b_1c_2}\varphi^{a_2b_2c_2}\varphi^{a_2b_2c_1}$, then we recover 5 index loops. Gluing two melonic graphs in this way gives the cut vertex graph scaling as $N^3(gN^{3/2})^{m_1+m_2}(g_pN^2)$. If $g_p \sim N^{-2}$, then this graph contributes at leading order in the large N limit [9, 11].
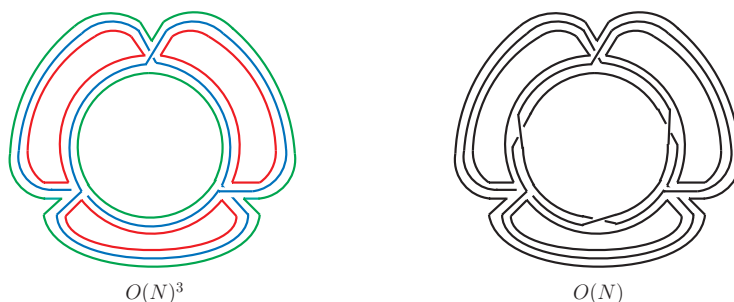
Figure 3. Order g^3 stranded diagrams for $O(N)^3$ and $O(N)$ theories. The diagram in the $O(N)^3$ theory has 6 loops and scales as $g^3 N^6$; the diagram in the $O(N)$ theory has 7 loops and scales as $g^3 N^7$.
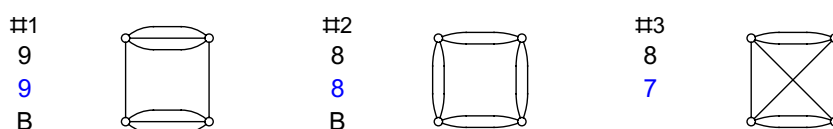

Figure 4. All vacuum diagrams of order g^4. The upper integer, shown in black, gives the leading power of N in the model of a symmetric traceless rank-3 tensor of $O(N)$; the lower integer, shown in blue, gives the leading power in the model of a tri-fundamental of $O(N)^3$. The letter B labels the bi-partite diagrams.
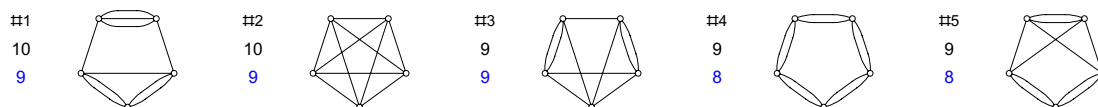
Figure 5. All vacuum diagrams of order g^5.

At order g^5 there are 5 distinct diagrams, which are shown in figure 5. Only the first two are suppressed just by $N^{-1/2}$: diagram #1 is a melon insertion into the unique graph of order g^3, while diagram #2 (the pentagram inscribed in a circle) is a new strcuture which appears at order g^5. Interestingly, at order g^7 there is no such new structure appearing, so that the only diagrams suppressed by $N^{-1/2}$ involve melonic insertions into the lower order diagrams.

Let us note that some g^8 graphs in the $O(N)$ theory are enhanced by N^2 compared to the $O(N)^3$ case. In some cases, this may be traced by to the fact that a diagram with an odd number of vertices, such as the g^3 diagram depicted in figure 3, may be enhanced by N. Cutting a propagator in such a graph and then gluing two of them gives diagram #8 of order g^6 in figure 6; it is indeed enhanced by N^2 compared to what is seen in the $O(N)^3$ theory. However, this diagram is still suppressed by N relative to the melonic ones. Indeed, in the large N limit where $g \sim N^{-3/2}$ the g^3 diagram is suppressed by $N^{-1/2}$ in the $O(N)$ model and by $N^{-3/2}$ in the $O(N)^3$ model. This translates into suppression of diagram #8 in figure 6 by N^{-1} and N^{-3}, respectively.
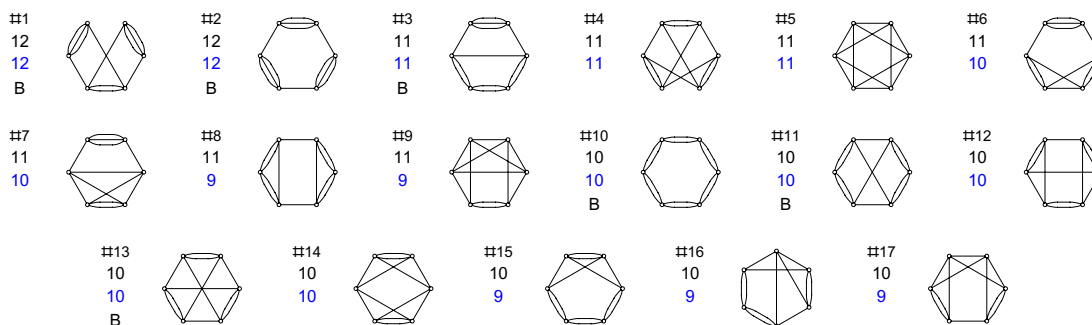
Figure 6. All vacuum diagrams of order g^6.

2.1 Antisymmetric tensor model

Another commonly used rank-3 representation of $O(N)$ is the fully anti-symmetric one. To modify our explicit calculations to the antisymmetric tensor model, we only have to change the index structure of the propagator to

$$\langle \phi^{abc} \phi^{a'b'c'} \rangle_0 = \frac{1}{6} \big(\delta^{aa'} \delta^{bb'} \delta^{cc'} + \delta^{ab'} \delta^{bc'} \delta^{ca'} + \delta^{ac'} \delta^{ba'} \delta^{cb'}$$
$$- \delta^{ab'} \delta^{ba'} \delta^{cc'} - \delta^{ac'} \delta^{bb'} \delta^{ca'} - \delta^{aa'} \delta^{bc'} \delta^{cb'} \big) , \quad (2.11)$$

while the vertex may still be taken to be of the tetrahedral form (2.6). We have carried out extensive perturbative calculations for this model too, and we find that each individual graph scales with N no faster than in the symmetric traceless model.[7] This provides evidence that the antisymmetric tensor model also has a melonic large N limit.

3 Bounds on the scaling

In the models of rank-3 tensor each propagator contains 3 strands. The strands are connected into closed loops, and the power of N for each graph is the total number of loops n. If n_L is the number of loops of length L, then

$$n = \sum_{L=2} n_L , \quad (3.1)$$

where we have excluded loops of length 1 which can only originate from snail diagrams. Since there are 12 stranded segments emanating from each quartic vertex, and each segment connects two vertices, the sum rule on the total number of stranded segments in a graph with m vertices is:

$$\sum_{L=2} L n_L = 6m . \quad (3.2)$$

The structure of the "tetrahedral" quartic vertex (1.1), where every pair of tensors has only one index in common, implies that no closed loop in the Feynman graph can be covered by

---

[7]For example, while all graphs of order g^2, g^4 and g^6 have the same leading powers of N as in the symmetric traceless model, graph #3 of order g^5 grows $\sim N^8$ in the antisymmetric model compared to $\sim N^9$ in the symmetric traceless model.
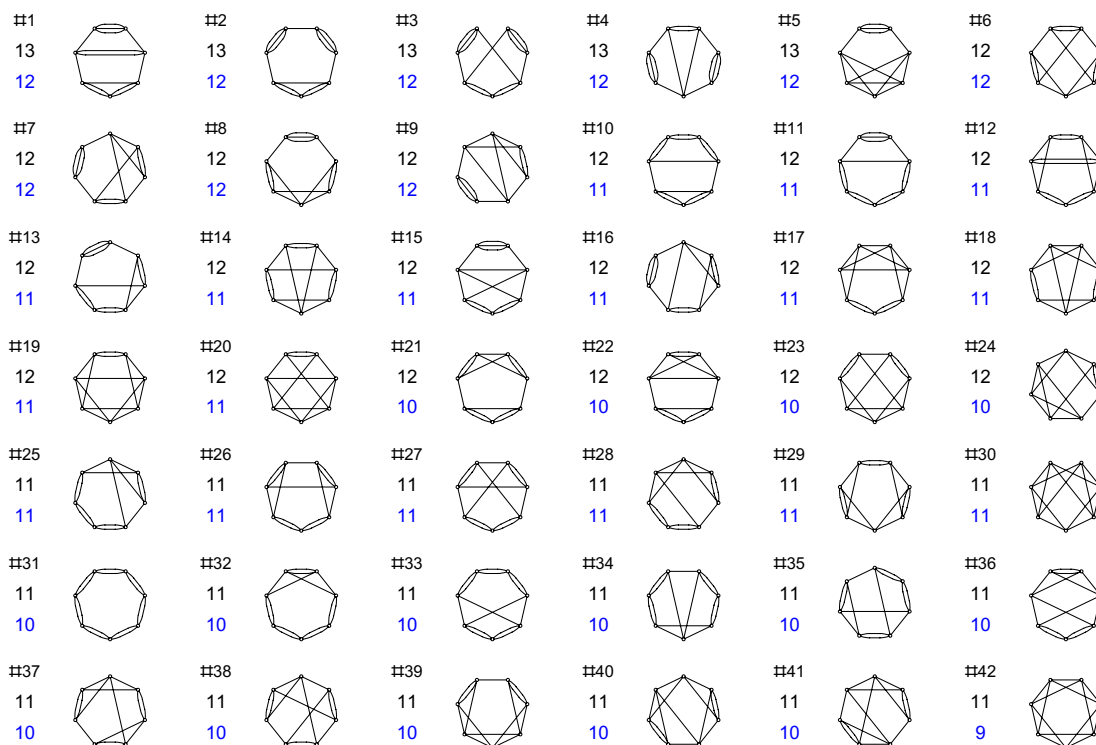
Figure 7. All vacuum diagrams of order g^7.

two different stranded loops (this would not be the case if the vertex had a pillow structure rather than tetrahedron). This puts an important constraint on the structure of possible stranded graphs.

For each melonic graph $n = 3 + 3m/2$. If the theory has a good melonic large N limit, then all other graphs scale with $n < 3 + 3m/2$. For the theory with $O(N)^3$ symmetry each strand has a distinct color, and it is possible to perform the counting by erasing one of the colors and relying on the topology of the double-line graphs. However, such a method is not available for the $O(N)$ theory where the strands are not distinguishable. This implies that there may be more possibilities for connecting the strands in the $O(N)$ case, so $n_{O(N)} \geq n_{O(N)^3}$. The explicit evaluation demonstrates that, for some graphs $n_{O(N)} - n_{O(N)^3}$ is positive. The maximum value of this quantity tends to increase with the order of perturbation theory: for graphs of order g^8 it is 2, while for graph #2 of order g^{12} it is 4 (see figure 11).

The sum rule (3.2) means that the maximization of n favors graphs with short index loops. As figure 2 shows, each melon insertion into a propagator adds three index loops of length 2, which is hard to beat.[8] On the other hand, if a Feynman graph contains few faces with perimeter less than 4, then (3.2) leads to a stringent upper bounds on its scaling. For example, if a graph has no faces with perimeter less than 4, then (3.2) implies that $n \leq 3m/2$, which means that the graph is suppressed at least by N^{-3} corresponding to the melonic graphs. This inequality is saturated only if $n_L = 0$ for $L > 4$, i.e. when all index

---

[8]Our explict results are consistent with the fact that a melon insertion in a graph always increases n by 3.
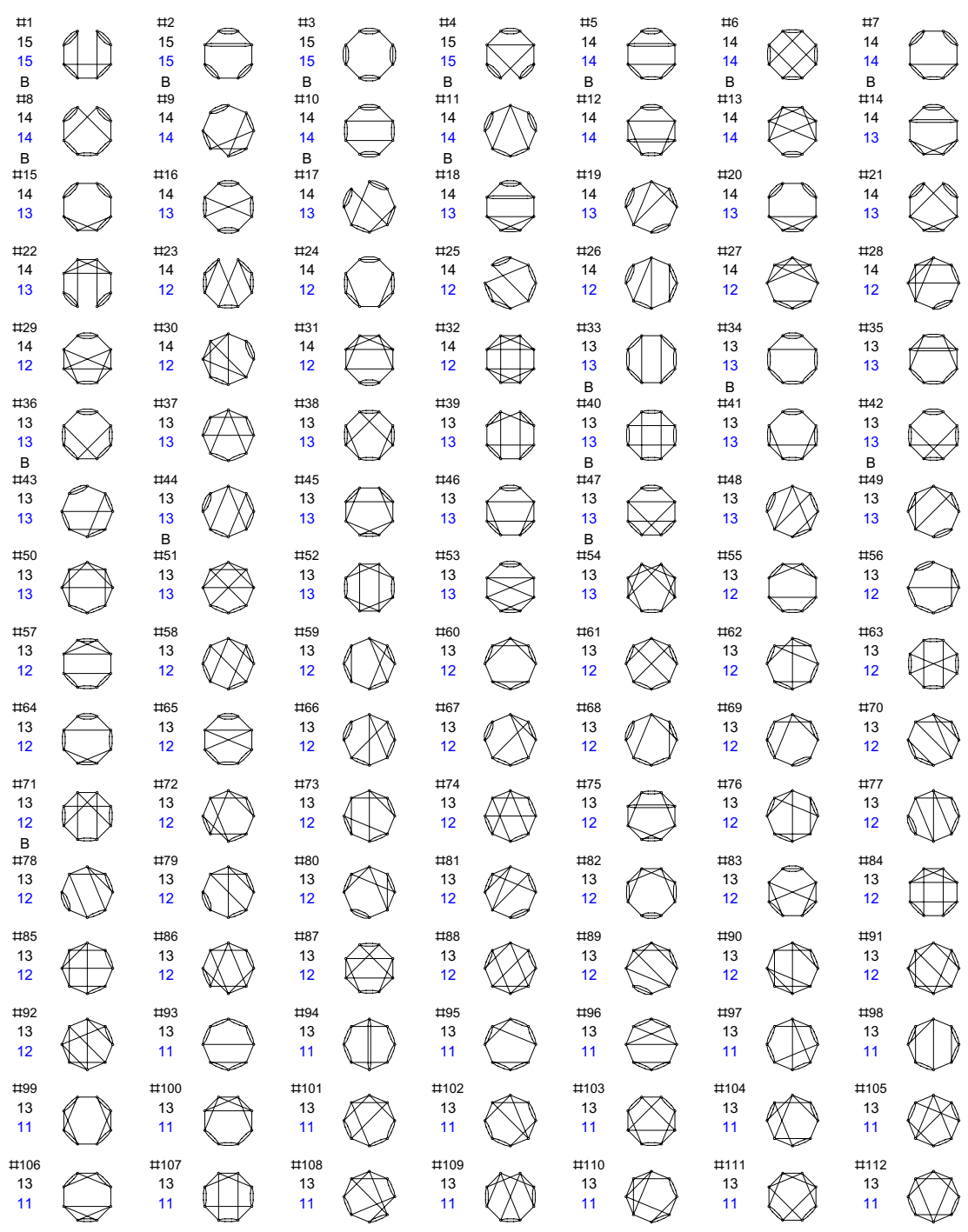
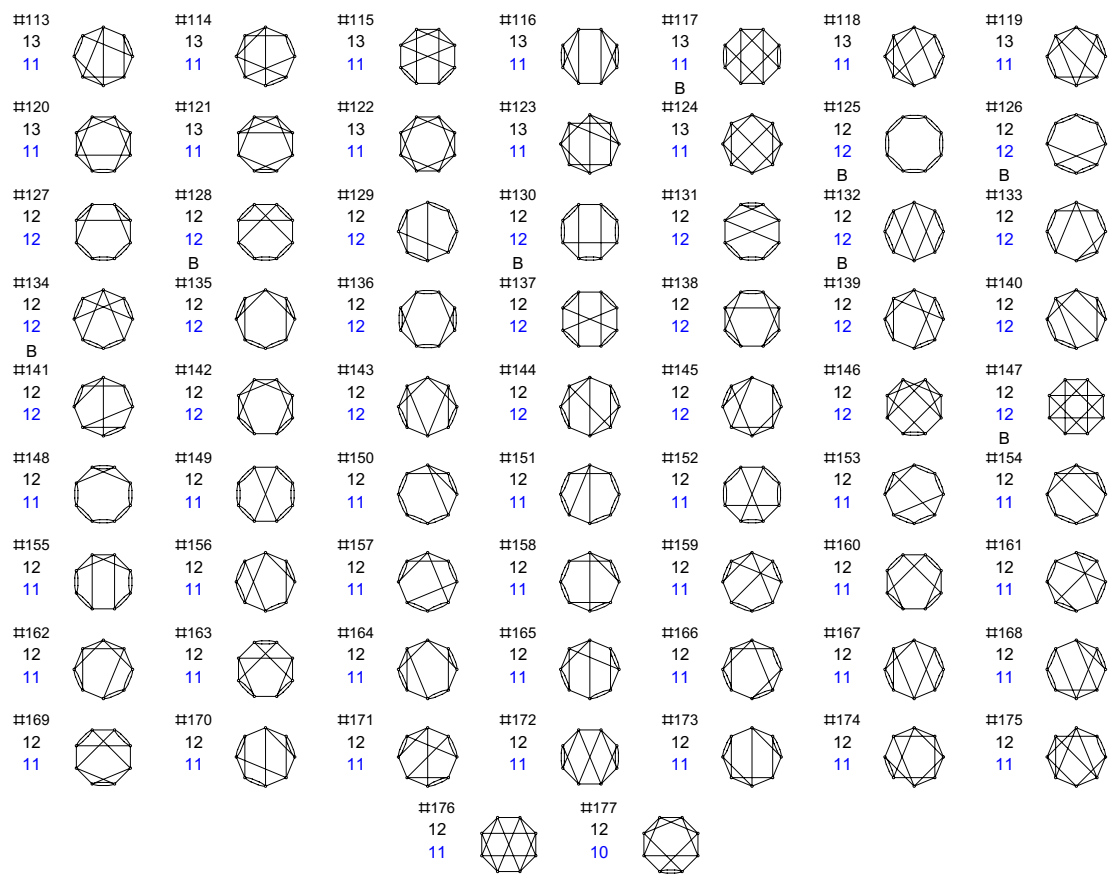**Figure 8**. (Part 1 of 2) All vacuum diagrams of order g^8.

Figure 8. (Part 2 of 2) All vacuum diagrams of order g^8.

loops have length 4. We notice that the octagram diagram ($\{8/3\}$ in the Schläfli notation for polygons), which is number #147 in figure 8, has no faces with perimeter shorter than 4. Our explicit calculation shows that the bound $n \leq 12$ is saturated for this graph; this means that each stranded loop has lengh 4.

More generally, if a Feynman graph has n_2 distinct faces of perimeter 2 and n_3 distinct faces of perimeter 3, we find the bound

$$\sum_{L=4} n_L \leq \frac{6m - 2n_2 - 3n_3}{4},\tag{3.3}$$

which implies

$$n \leq \frac{n_2}{2} + \frac{n_3}{4} + \frac{3m}{2},\tag{3.4}$$

and the equality may hold only if the r.h.s. is an integer. A graph may survive in the melonic large N limit only if $\frac{n_2}{2} + \frac{n_3}{4}$ is ≥ 3. This is not the case for many non-melonic graphs.

The bound (3.4) is often quite informative. For example, for the pentagram graph, which is diagram #2 in figure 5, we find $n_2 = 0, n_3 = 10$, so that $n \leq 10$. The explicit calculation shows that this bound is saturated. As a result, the pentagram graph is suppressed only by $N^{-1/2}$ in the melonic limit. Moving on to the graphs of order g^8, for graph
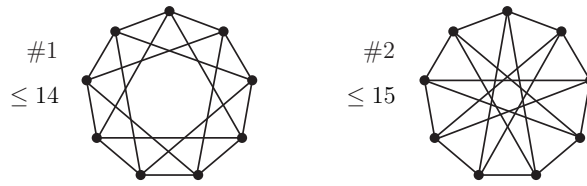
Figure 9. Polygon diagrams {9/3} and {9/4} inscribed in a circle. The numbers refer to the power of N in the $O(N)$ model.

#176 we find by inspection that $n_2 = 0, n_3 = 4$ so that the bound (3.4) is $n \leq 13$. The direct calculation gives $n = 12$, one unit below the bound. For graph #32 we find by inspection that $n_2 = 0, n_3 = 8$ so that the bound (3.4) is $n \leq 14$, and the direct calculation gives $n = 14$. For graph #122 in figure 8 we find by inspection that $n_2 = 0, n_3 = 8$ so that the bound (3.4) is $n \leq 14$, and the direct calculation gives $n = 13$; and so on.

The bound (3.4) is particularly easy to apply to the bipartite graphs, which have $n_3 = 0$. For example, for graph #6 of order g^8, which is bipartite, $n_2 = 4$ and the bound is $n \leq 14$. The direct calculation gives $n = 14$, so that the bound is saturated. Similarly, for graph #117 of order g^8, $n_2 = 2$ and the bound is $n \leq 13$; the direct calculation shows that the bound is saturated.

While the bound (3.4) is useful in many cases, it does not provide a proof of the melonic scaling. For example, for graph #125 in figure 8, $n_2 = 8, n_3 = 0$, so that the bound (3.4) is $n \leq 16$. The actual result $n = 12$ is far from saturating this bound. This is a typical situation for the bubble graphs, of which #125 is an example. For example, for a bubble graph with m vertices, $n_2 = m$, so that the bound reads $n \leq 4m$. However, the actual scaling is found to be $n = m + 4$, which is far less than the bound at large m.

4 Beyond the eighth order

A complete study at any order beyond g^8 requires calculating the combinatorics of a prohibitive number of graphs, and we have not carried out this task completely. We have, however, used a combination of direct calculations and the bounds (3.4) to make some checks of higher order diagrams.

At order g^9 one of the most symmetric star shapes is {9/3} (in the Schläfli notation) inscribed in a circle. This diagram, shown on the left in figure 9, consists of three mutually rotated equilateral triangles, and one may wonder if its contriubtion is relatively enhanced similarly to that of the pentagram. However, since $n_2 = 0$ and $n_3 = 3$, we find the bound $n \leq 14$. So, without any direct calculation we see that the diagram is suppressed at least by $N^{-5/2}$ compared to the melonic ones.

For the {9/4} inscribed in a circle we have $n_2 = 0$ and $n_3 = 9$, so that the bound (3.4) gives $n \leq 15$. This means that the diagram is suppressed at least by $N^{-3/2}$ compared to the melonic ones.

We have also studied the class of polygons {m/2} (in the Schläfli notation) inscribed in a circle. For $m = 5$ this is the pentagram, for $m = 7$ it is graph #42 in figure 7, and for $m = 9, 11, 13, 15$ the graphs are shown in figure 10. With the exception of $m = 7$ we
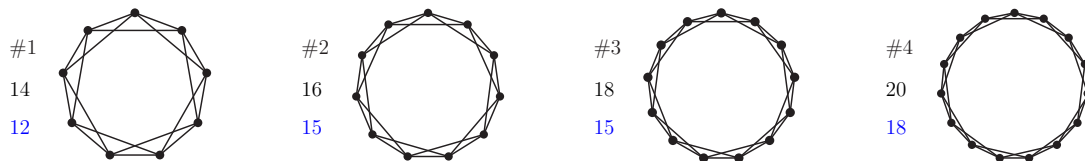
Figure 10. A family of polygon diagrams $\{m/2\}$ inscribed in a circle for $m = 9, 11, 13, 15$. The numbers refer to the power of N in the $O(N)$ model.
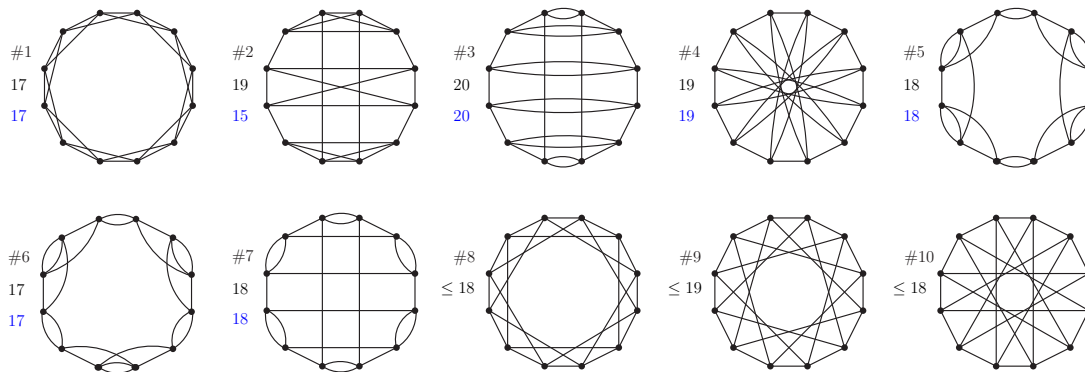

Figure 11. Some non-melonic g^{12} diagrams. They are all suppressed compared to the melonic ones which scale as N^{21}.

find the result $n = m + 5$, which shows a linear growth of the scaling with the number of vertices, similarly to the bubble graphs (for $m = 7$ we instead find a smaller value $n = 11$).

We have also checked a few graphs at order g^{12}; see figure 11. None of these non-melonic graphs scale as fast as the melonic graphs, which are $\sim g^{12}N^{21}$. Some graphs, like $\#8, \#9, \#10$, did not need to be calculated explicitly because the upper bound (3.4) shows they are not competitive with the melonic ones. For graph $\#2$ we observe an enhancement by N^4 compared to the $O(N)^3$ theory, but the graph is still suppressed by N^{-2} compared to the melonic ones.

5 Melonic graphs

Let us define normalized interaction terms in the $O(N)^3$ and $O(N)$ cases

$$V_{O(N)^3} = \frac{1}{4}\tilde{g}\varphi^{abc}\varphi^{ade}\varphi^{fbe}\varphi^{fdc}, \qquad V_{O(N)} = \frac{3}{2}g\phi^{abc}\phi^{ade}\phi^{fbe}\phi^{fdc}, \tag{5.1}$$

where the rank 3 tensor field φ^{abc} has distinguishable indices, while ϕ^{abc} is a symmetric traceless tensor. For the $O(N)^3$ theory the sum over connected melonic vacuum graphs in the large N limits is

$$F_{O(N)^3} = N^3\left(\sum_{n=1}^{\infty} a_{2n}\tilde{\lambda}^{2n}\right), \tag{5.2}$$

where $\tilde{\lambda}^2 = \tilde{g}^2N^3$. The specific coefficients a_{2n} depend on the dimensionality and the field content of the theory. For example, for a scalar theory in $d = 0$,

$$a_2 = \frac{1}{8}, \quad a_4 = \frac{1}{4}, \quad a_6 = \frac{11}{12}, \quad a_8 = \frac{35}{8}, \quad \ldots, \quad a_{2n} = \frac{1}{8n(4n+1)}\binom{4n+1}{n}. \tag{5.3}$$

These coefficients can be obtained by solving Schwinger-Dyson equation for the two-point function in the $d = 0$ dimension [8]

$$G_{\text{melons}}(\lambda) = 1 + \lambda^2 G_{\text{melons}}(\lambda)^4. \tag{5.4}$$

Then free energy F is obtained from G_{melons} through the relation $G_{\text{melons}} = 1 + 4\lambda \partial_\lambda F/N^3$.

Now, if we assume that in the large N limit melonic graphs dominate also in the $O(N)$ model, then we expect to find the same expression in terms of the coupling $\lambda^2 = g^2 N^3$, up to an overall factor:

$$F_{O(N)} = \frac{N^3}{6} \left(\sum_{n=1}^{\infty} a_{2n} \lambda^{2n} \right). \tag{5.5}$$

The reason for the factor $1/6$ is that the number of degrees of freedom in the symmetric traceless rank 3 tensor is $N(N+4)(N-1)/6 = N^3/6 + O(N^2)$. We explicitly checked (5.5) up to order λ^8. So, the melonic limits in the $O(N)$ and $O(N)^3$ models are simply related.

Acknowledgments

References

[1] J. Ambjørn, B. Durhuus and T. Jonsson, *Three-dimensional simplicial quantum gravity and generalized matrix models*, *Mod. Phys. Lett.* **A 6** (1991) 1133 [INSPIRE].

[2] N. Sasakura, *Tensor model for gravity and orientability of manifold*, *Mod. Phys. Lett.* **A 6** (1991) 2613 [INSPIRE].

[3] M. Gross, *Tensor models and simplicial quantum gravity in > 2 − D*, *Nucl. Phys. Proc. Suppl.* **25A** (1992) 144 [INSPIRE].

[4] R. Gurau, *Colored group field theory*, *Commun. Math. Phys.* **304** (2011) 69 [arXiv:0907.2582] [INSPIRE].

[5] R. Gurau and J.P. Ryan, *Colored tensor models — A review*, *SIGMA* **8** (2012) 020 [arXiv:1109.4812] [INSPIRE].

[6] R. Gurau and V. Rivasseau, *The 1/N expansion of colored tensor models in arbitrary dimension*, *EPL* **95** (2011) 50004 [arXiv:1101.4182] [INSPIRE].

[7] R. Gurau, *The complete $1/N$ expansion of colored tensor models in arbitrary dimension*, *Annales Henri Poincaré* **13** (2012) 399 [`arXiv:1102.5759`] [ɪɴSPIRE].

[8] V. Bonzom, R. Gurau, A. Riello and V. Rivasseau, *Critical behavior of colored tensor models in the large-N limit*, *Nucl. Phys.* **B 853** (2011) 174 [`arXiv:1105.3122`] [ɪɴSPIRE].

[9] A. Tanasa, *Multi-orientable group field theory*, *J. Phys.* **A 45** (2012) 165401 [`arXiv:1109.0694`] [ɪɴSPIRE].

[10] V. Bonzom, R. Gurau and V. Rivasseau, *Random tensor models in the large-N limit: uncoloring the colored tensor models*, *Phys. Rev.* **D 85** (2012) 084037 [`arXiv:1202.3637`] [ɪɴSPIRE].

[11] S. Carrozza and A. Tanasa, *$O(N)$ random tensor models*, *Lett. Math. Phys.* **106** (2016) 1531 [`arXiv:1512.06718`] [ɪɴSPIRE].

[12] A.Z. Patashinskii and V.L. Pokrovskii, *Second order phase transitions in a Bose fluid*, *JETP* **19** (1964) 677.

[13] C. de Calan and V. Rivasseau, *The perturbation series for ϕ^4 in three-dimensions field theory is divergent*, *Commun. Math. Phys.* **83** (1982) 77 [ɪɴSPIRE].

[14] G. 't Hooft, *A Planar Diagram Theory for Strong Interactions*, *Nucl. Phys.* **B 72** (1974) 461 [ɪɴSPIRE].

[15] E. Brézin, C. Itzykson, G. Parisi and J.B. Zuber, *Planar diagrams*, *Commun. Math. Phys.* **59** (1978) 35 [ɪɴSPIRE].

[16] E. Witten, *An SYK-like model without disorder*, `arXiv:1610.09758` [ɪɴSPIRE].

[17] I.R. Klebanov and G. Tarnopolsky, *Uncolored random tensors, melon diagrams and the Sachdev-Ye-Kitaev models*, *Phys. Rev.* **D 95** (2017) 046004 [`arXiv:1611.08915`] [ɪɴSPIRE].

[18] S. Sachdev and J. Ye, *Gapless spin fluid ground state in a random, quantum Heisenberg magnet*, *Phys. Rev. Lett.* **70** (1993) 3339 [`cond-mat/9212030`] [ɪɴSPIRE].

[19] O. Parcollet and A. Georges, *Non-Fermi-liquid regime of a doped Mott insulator*, *Phys. Rev.* **B 59** (1999) 5341 [`cond-mat/9806119`].

[20] A. Georges, O. Parcollet and S. Sachdev, *Mean field theory of a quantum Heisenberg spin glass*, *Phys. Rev. Lett.* **85** (2000) 840 [`cond-mat/9909239`].

[21] A. Kitaev, *A simple model of quantum holography*, talk given at *KITP Program: Entanglement in Strongly-Correlated Quantum Matter*, April 6–July 2, KITP, Santa Barbara, U.S.A. (2015); Part 1 and Part 2 available online.

[22] J. Polchinski and V. Rosenhaus, *The spectrum in the Sachdev-Ye-Kitaev model*, *JHEP* **04** (2016) 001 [`arXiv:1601.06768`] [ɪɴSPIRE].

[23] J. Maldacena and D. Stanford, *Remarks on the Sachdev-Ye-Kitaev model*, *Phys. Rev.* **D 94** (2016) 106002 [`arXiv:1604.07818`] [ɪɴSPIRE].

[24] A. Jevicki, K. Suzuki and J. Yoon, *Bi-local holography in the SYK model*, *JHEP* **07** (2016) 007 [`arXiv:1603.06246`] [ɪɴSPIRE].

[25] D.J. Gross and V. Rosenhaus, *A generalization of Sachdev-Ye-Kitaev*, *JHEP* **02** (2017) 093 [`arXiv:1610.01569`] [ɪɴSPIRE].

[26] F. Ferrari, *The large D limit of planar diagrams*, `arXiv:1701.01171` [ɪɴSPIRE].

[27] M. Beccaria and A.A. Tseytlin, *Partition function of free conformal fields in 3-plet representation*, *JHEP* **05** (2017) 053 [arXiv:1703.04460] [INSPIRE].

[28] H. Kleinert, A. Pelster, B.M. Kastening and M. Bachmann, *Recursive graphical construction of Feynman diagrams and their multiplicities in phi**4 theory and in $\phi^2 A$ theory*, *Phys. Rev.* **E 62** (2000) 1537 [hep-th/9907168] [INSPIRE].